

# Accurate parameter estimation of Au/GaN/GaAs Schottky diode model using grey wolf optimization

A. Rabehi<sup>a,c,d</sup>, A. Douara<sup>b</sup>, A. Rabehi<sup>c</sup>, H. Helal<sup>d</sup>, A. Memdouh Younsi<sup>c</sup>,  
M. Amrani<sup>a</sup>, I. E. Abbas<sup>d</sup>, E. Comini<sup>d</sup>, and Z. Benamara<sup>a</sup>

<sup>a</sup>Laboratoire de Micro-Electronique Appliquée,  
Université Djillali Liabès de Sidi Bel Abbès, BP 89, 22000, Sidi Bel Abbès, Algeria.

<sup>b</sup>Faculty of Science and Technology, Tissemsilt University, Algeria.

<sup>c</sup>Telecommunications and Smart Systems Laboratory, University of Djelfa, PO Box 3117, Djelfa 17000, Algeria.

<sup>d</sup>Sensor Laboratory University of Brescia, Via D. Valotti 9, 25133 Brescia, Italy.

Received 27 September 2023; accepted 20 December 2023

The Au/GaN/GaAs Schottky diode is a fundamental electronic component with versatile applications. In this study we delve into the parameter estimation of Au/GaN/GaAs Schottky diodes using the Grey Wolf Optimizer (GWO) algorithm. Our research encompasses experimental procedures, mathematical modeling, and optimization techniques to extract critical electrical parameters, including the ideality factor ( $n$ ), Schottky barrier height ( $\phi_{bn}$ ), and series resistance ( $R_S$ ). The primary aim is to enhance our comprehension of the behavior of Au/GaN/GaAs Schottky diodes and showcase the effectiveness of GWO in achieving precise parameter estimates. These diodes, featuring metal-semiconductor junctions, play pivotal roles in electronics, necessitating accurate parameter determination for optimized functionality. The effectiveness of the GWO algorithm was examined through a comparative analysis, employing analytical techniques pioneered by Cheung and Cheung. This study sought to assess the algorithm's performance and accuracy in parameter estimation for Au/GaN/GaAs Schottky diodes, providing valuable insights into its practical applicability in electronic device characterization and optimization. Keywords: Schottky diodes, Grey Wolf Optimization, Electrical measurement. Parameter estimation, GaN, GaAs

*Keywords:* Schottky diodes; grey wolf optimization; electrical measurement; parameter estimation; GaN; GaAs.

DOI: <https://doi.org/10.31349/RevMexFis.70.021004>

## 1. Introduction

Semiconductor devices, such as Schottky diodes, constitute the bedrock of modern electronics and optoelectronics, playing pivotal roles in diverse applications ranging from power rectification to photodetection in cutting-edge optoelectronic systems [1–3]. Precise characterization and parameter estimation of these devices are of paramount importance to ensure their optimal performance and further advance electronic technologies.

The analysis of current-voltage (I-V) characteristics is a fundamental step in understanding semiconductor device behavior. In industrial contexts, microelectronic chip manufacturers heavily rely on rigorous I-V characterization as a cornerstone of quality assurance for their semiconductor chips [4].

Among the key parameters extracted from I-V characteristics, the ideality factor  $n$ , barrier height  $\phi_{bn}$ , and series resistance  $R_S$  of Schottky diodes hold critical significance [5, 6]. Researchers and engineers require these parameters for the effective design and optimization of microelectronic components [5, 7, 8].

Over the years, several methodologies have been developed to determine these Schottky diode parameters. Traditional approaches, although effective to some extent, often fall short when addressing complex factors such as series resistance. Alternative models, such as Norde's thermionic

emission-based approach [9] and techniques employed by Cheung and Cheung [10], provide valuable insights but are frequently characterized by stepwise procedures that assume limited interactions between parameters. To overcome these limitations and the dependence on simplifying assumptions, artificial intelligence (AI) techniques have found their way into semiconductor device analysis and parameter extraction [11, 12]. Among these techniques, evolutionary algorithms (EAs) have emerged as powerful tools for modeling and optimizing semiconductor devices [13, 14].

The Grey Wolf Optimization (GWO) algorithm, a member of the EA family [15], has gained attention for its stochastic and versatile approach to optimizing complex, multi-dimensional problems. Unlike traditional numerical analyses, GWO excels in handling nonlinear systems without prior knowledge of derivatives and offers robust performance across diverse parameter settings.

This study embarks on a journey to leverage the potential of the GWO algorithm in the context of Au/GaN/GaAs Schottky diodes. By introducing this optimization algorithm to the realm of diode parameter estimation, we aim to unravel the intricacies of Schottky diode behavior and explore novel avenues for enhancing their performance.

Through rigorous comparative analyses with established methods, we demonstrate the GWO algorithm's exceptional accuracy in determining diode parameters, reaffirming its credibility as a robust optimization tool. Furthermore, its

simplicity and adaptability open doors for further research and development in semiconductor applications.

Moreover, GWO has proven to be a valuable tool in diverse optimization problems. For instance, researchers like Abushawish *et al.*, [16] utilized GWO to extract physical parameters associated with the active layer of Gallium Nitride GaN high electron mobility transistors (HEMTs) fabricated on Silicon Si substrates. In a different context, H. Bencherif *et al.*, [17] demonstrated GWO's application in improving the efficiency of a-Si:H/c-Si thin heterojunction solar cells. Additionally, Hülya Doğan *et al.*, [18] applied GWO to extract physical parameters of Al/p-Si Schottky Barrier Diode. This wealth of applications attests to the versatility and effectiveness of GWO across various semiconductor devices.

This paper offers a comprehensive exploration of the methodology, results, and broader implications of integrating the GWO algorithm into Schottky diode parameter estimation. It seeks to provide a holistic understanding of how this innovative approach can elevate the efficiency and performance of electronic devices, marking a significant stride in the pursuit of cutting-edge semiconductor technology.

## 2. Experimental procedure

### 2.1. Sample preparation

The GaAs homoepitaxial layer, grown using the RIBER 32 MBE system, developed a native oxide layer upon exposure to air. The sample preparation process included the following steps [16–19]:

- **Chemical Cleaning:** The samples underwent a thorough cleaning process, which involved sequential immersion in  $\text{H}_2\text{SO}_4$ , deionized water, and both cold and hot methanol. Throughout this process, ultrasonic treatment was applied to enhance the cleaning efficacy. The final step included thorough drying using nitrogen gas  $\text{N}_2$ .
- **Nitridation:** Nitridation was carried out using a GDS  $\text{N}_2$  plasma source operating within a power range of 5-10 W. The nitrogen pressure was maintained at approximately  $10^{-1}$  Pa, and exposure times ranged from 0 to 60 minutes. It is noteworthy that all nitridation steps were conducted within the same Ultra-High Vacuum (UHV) chamber.

### 2.2. Nitridation process and GaN layer formation

The nitridation process employed for GaAs substrates relies on the presence of metallic gallium crystallites created during surface cleaning through ion bombardment. Subsequent to the formation of gallium crystallites, the substrate surface undergoes exposure to an active nitrogen flux ( $\text{N}$ ,  $\text{N}^+$ ,  $\text{N}_2^+$ ), generated by a discharge source known as the Glow Discharge Cell (GDS). The GDS source operates within a power

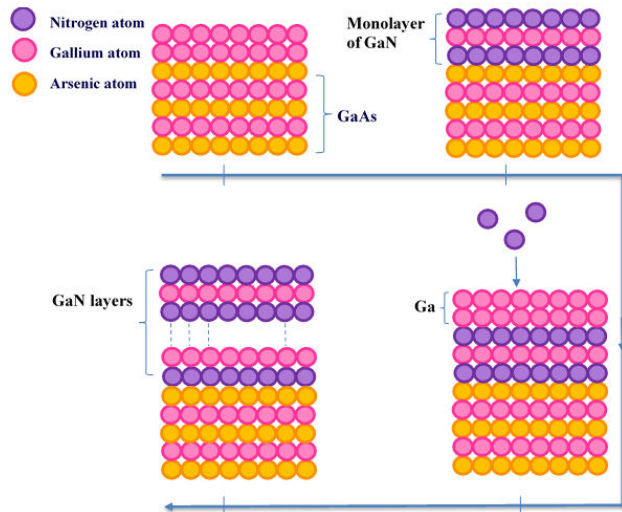


FIGURE 1. Schematic representation of the different stages of the nitridation process for the formation of monolayers of GaN/GaAs.

range of 3 to 1, with plasma exposure times ranging from 0 to 60 minutes, and temperatures varying from 450 to 620°C.

Figure 1 schematically illustrates the evolving states of the GaAs substrate surface during distinct nitridation processes, as inferred from results obtained through electronic spectroscopies [19, 20]. In this process, nitrogen atoms combine with metallic gallium atoms present on the ion-bombarded surface of GaAs. Monolayers of gallium act as precursors, initiating the subsequent formation of GaN layers through the controlled consumption of gallium under optimal growth conditions, which include substrate temperature, the angle of nitrogen flux incidence, nitridation time, among others.

Consequently, the GaAs surface transforms, becoming adorned with layers of GaN. Noteworthy is the facile method to augment the thickness of the GaN layer, achieved by depositing a layer of gallium on the surface and iteratively repeating the nitridation step.

### 2.3. Characterization Techniques

While XPS, XRD, and MEB characterization techniques are powerful tools for providing insights into the morphological and structural properties of semiconductor structures [21], [22], it is essential to note that our investigation primarily focuses on parameter extraction. For a more in-depth analysis of the structural and morphological aspects, we recommend referring to the detailed studies conducted in recent works [19, 20].

### 2.4. Sample Preparation and Annealing Conditions

Table I summarizes the preparation procedure for samples A and B, encompassing the cleaning, nitridation, thickness of GaN, and annealing operation.

TABLE I. Preparation procedure of samples.

Sample	Cleaning	Nitridation	Thickness of GaN	Annealing Operation
A	Chemical+ionic	500 °C, 5 min, p=5 W	0.7 nm with 2% of oxygen	620°C at 60 min
B	Chemical+ionic	500 °C, 30 min, p=5 W	2 nm with 2% of oxygen	620°C at 60 min

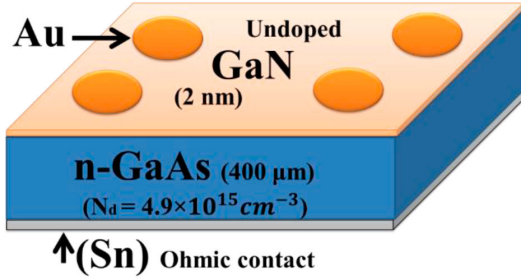


FIGURE 2. Schematic diagram of the elaborated Au/n-GaN/GaAs Schottky diodes.

These GaAs substrates (100) are n type, with a concentration of  $N_d = 4.9 \times 10^{15} \text{ cm}^{-3}$ , and possess a thickness of  $400 \pm 20 \mu\text{m}$ .

Both samples were subjected to the same annealing conditions, involving a temperature of  $620^\circ\text{C}$  for 60 minutes. This annealing process, as a heat treatment step, significantly influences the crystalline structure and defect density of the material [3].

### 2.5. Electrical characteristics and measurement methodology

To establish Ohmic contact, SN (metal) was employed, and the electrical characteristics of the structures were assessed using Au probes as temporary gate contacts, with a contact area denoted as  $S = 4.41 \times 10^{-3} \text{ cm}^2$ . The schematic view of the elaborated Au/GaN/n-GaAs Schottky diodes is illustrated in Fig. 2. The I-V (current-voltage) measurements were conducted through a conventional methodology, utilizing an HP4155B instrument. All measurements were carried out at room temperature and in the absence of external light sources.

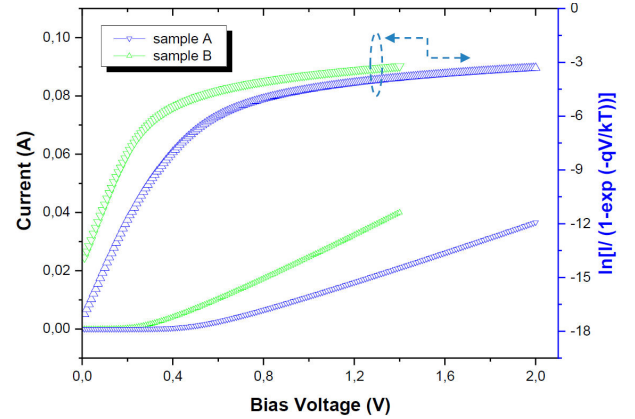
## 3. I (V) Characteristic

In the context of an ideal schottky barrier diode (SBD), it is assumed that the forward bias current of the device primarily arises from thermionic emission. This current can be mathematically expressed as [23–25],

$$I = I_0 (\exp [\{q(V - IR_s)\} / nkT] - 1), \quad (1)$$

where

$$I_0 = AA^*T^2 \exp(-[q\phi_{bn}]/kT). \quad (2)$$


 FIGURE 3. Current-voltage characteristic and the evolution of  $f(V) = \text{Ln}[I/(1 - \exp(-qV)/kT)]$ .

Here are the meanings of the symbols used in these equations:  $I_0$  the saturation current,  $V$  represents the bias voltage,  $I$  stands for the diode current,  $A$  denotes the diode area,  $A^*$  represents the Richardson constant (for GaAs is  $8.16 \text{ A cm}^{-2} \text{ k}^{-2}$  [26]),  $q$  signifies the electron charge,  $T$  corresponds to the absolute temperature, and  $k$  stands for the Boltzmann constant. The ideality factor  $n$ , Schottky barrier height  $\phi_{bn}$  and series resistance  $R_s$  are intrinsic parameters of the SBD. Precise determination of these parameters is crucial and is typically achieved through the analysis of experimental I-V characteristics. For visual reference, Fig. 3 show the I-V characteristics of the Au/GaN/n-GaAs Schottky diode.

The  $f(V)$  curve depicted in Fig. 1 exhibits two linear segments, with a transitional segment in between. In the first linear region, we can determine the ideality factor  $n$  and the saturation current  $I_0$  by examining the slope and intercept of the plot on the current axis. The alteration in slope in the  $f(V)$  characteristic caused by the effect of the series resistance  $R_s$ . By using these approximations and analyzing the region II, the found results are given in Table II.

The Schottky diode parameters as the barrier height  $\phi_{bn}$ , the ideality factor  $n$ , and the series resistance  $R_s$  were also achieved using a method developed by Cheung and Cheung and confirmed by Werner [10, 27]. The values of the series resistance can be determined from the following functions:

$$\frac{\partial V}{\partial(\ln I)} = \frac{nKT}{q} + IR_s. \quad (3)$$

According to Eq. (3), the slope of a linear portion of  $dV/d\ln(I)$  versus  $I$  gives the  $R_s$  series resistance and its

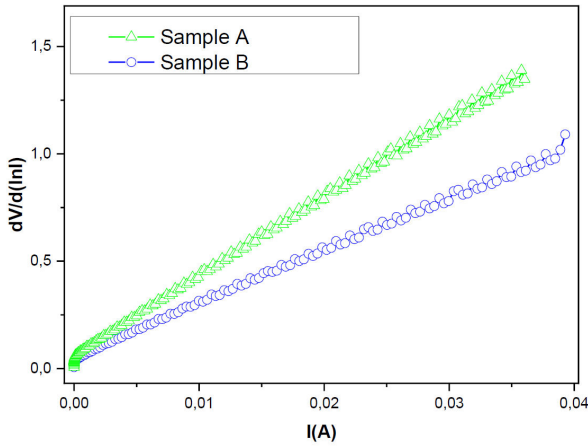


FIGURE 4. The  $dV/d \ln(I)$  vs.  $I$  plot of Au/GaN/GaAs Schottky diode.

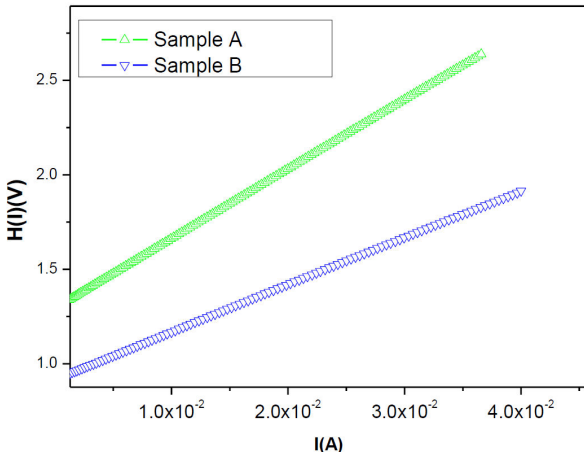


FIGURE 5. The  $H(I)$  vs.  $I$  plot of Au/GaN/GaAs Schottky diode.

intercept on the current axis gives  $nkT/q$ . To obtain barrier height, Cheung and Cheung defined a function as:

$$H(I) = V - \left( \frac{nKT}{q} \right) \ln \left( \frac{I}{AA^*T^2} \right) = n\phi_b + IR_S. \quad (4)$$

Using the value of ideality factor determined from Eq. (3), a plot of  $H(I)$  versus  $I$  also yields a straight line, with a  $y$ -axis intercept that equals to  $n\phi_{bn}$ . The slope of this plot allows a second determination of  $R_S$  that can be used to check the consistency of this approximation. The plots of  $dV/d(\ln I) - I$  and  $H(I) - I$  are shown in Fig. 4 and 5. The obtained values are shown in Table III; the results show the consistency of the method.

## 4. Parameter Estimation with Grey wolf optimizer

### 4.1. Parameter estimation

The process of estimating the model parameters for the Schottky-barrier diode employs a systematic approach. To

initiate this procedure, we begin by gathering a comprehensive dataset of experimental I-V characteristics that specifically pertain to the Schottky-barrier diode. Following this data collection, we employ the highly efficient Grey Wolf Optimizer (GWO) to meticulously fine-tune these model parameters. The primary goal is to achieve precise alignment between these parameters and the empirical data, ensuring a smooth convergence with the intricate dynamics described by Eq. (1). Equation (1) represents a profoundly complex and nonlinear mathematical relationship, presenting substantial challenges for direct analytical solutions. Given this intricacy, we undertake the task of transforming the Schottky-barrier diode model, as defined by Eq. (1), into a more accessible and manageable form, denoted as Eq. (5). This transformation facilitates a more effective analysis and streamlines the parameter optimization process [28].

$$\begin{aligned} y(I, V, \theta) &= I - I_0 [\exp(q(V - IR_S)/nkT) - 1] \\ &= f(I, V, \theta). \end{aligned} \quad (5)$$

In a practical system, the parameters  $\theta = [\phi_{bn}, n, R_S]$  are initially unknown and need to be determined with maximum precision. The task of parameter estimation can be conceptualized as the minimization of the root-mean-square error (RMSE), which serves as our fitness function and is articulated as follows [29]:

$$e = \sqrt{\frac{1}{L} \sum_{j=1}^L [y(I_j, V_j, \theta)]^2}, \quad (6)$$

where  $I_j$  and  $V_j$  represent the experimental current-voltage data points, respectively, with  $L$  denoting the total number of experimental data points. The model parameters, denoted as  $\theta$ , have been defined previously.

Our primary goal is to minimize the value of  $e$  in Eq. (6), striving to reduce it as close to zero as feasible. Subsequently, the parameters  $\theta$  can be accurately determined by employing the proposed GWO. Notably, this optimization technique relies solely on evaluating the fitness value to guide its search and does not necessitate derivatives of the system.

### 4.2. GWO algorithm

The GWO algorithm, a meta-heuristic approach, has gained widespread application in solving various optimization problems in recent times [15]. This innovative method draws inspiration from the social organization and hunting strategies of gray wolves, cleverly mimicking their behavior in problem-solving [30]. Gray wolves are known for their pack-hunting strategy, and Fig. 6 provides insight into the hierarchical structure within a wolf pack. This hierarchical arrangement is led by the alpha wolf denoted as  $\alpha$ , responsible for presenting the most optimal solution in the GWO method's mathematical formulation. Subsequently, the beta wolf, represented as  $\beta$ , follows  $\alpha$ , and the delta and omega wolves,

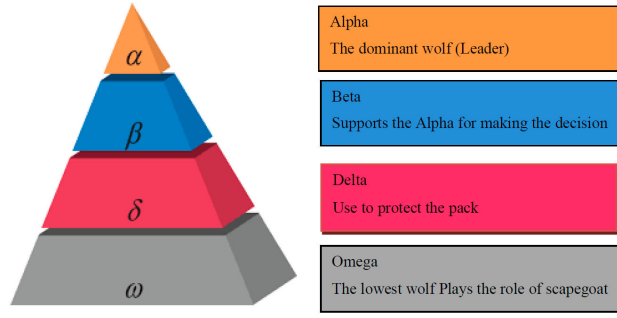


FIGURE 6. Hierarchy of Grey Wolf.

$\delta$  and  $\omega$ , respectively, trail behind  $\beta$ , each contributing to the mathematical representation of alternative solutions.

During the hunting process, gray wolves employ a strategy akin to encircling their prey, which is mathematically defined by Eqs. (7) and (8) [15]:

$$\vec{D} = \left| \vec{C} \cdot \vec{X}_p(t) - \vec{X}(t) \right|, \quad (7)$$

$$\vec{X}(t+1) = \vec{X}_p(t) - \vec{A} \cdot \vec{D}. \quad (8)$$

Here,  $t$  represents the current iteration value,  $\vec{A}$  and  $\vec{C}$  denote coefficient vectors,  $\vec{X}_p$  is the location vector of the prey,  $\vec{X}$  represents the location vector of a gray wolf.

The vectors  $\vec{A}$  and  $\vec{C}$  are calculated using the following equations:

$$\vec{A} = 2\vec{a} \cdot \vec{r}_1 - \vec{a}, \quad (9)$$

$$\vec{C} = 2\vec{r}_2. \quad (10)$$

The value of  $\vec{a}$  in these equations linearly decreases from 2 to 0 depending on the number of rounds. The variables  $\vec{r}_1$  and  $\vec{r}_2$  take on random values within the range of [0-1].

The hunting behavior of gray wolves can be described through two primary strategies, as follows:

### Hunting

During the hunting process, gray wolves exhibit remarkable coordination and tracking abilities. In a wolf pack, the alpha wolf often assumes the role of leading the pursuit, although there are instances when other wolves also take the lead. The alpha's position as the leader is strategic since it is typically the closest wolf to the prey, allowing it to possess the most accurate information about the prey's location. This information guides the pack's hunting strategy. The GWO algorithm employs a similar concept: it records the first best solution found during the hunting process, similar to the alpha wolf's role. Subsequently, all agents, including omega, adapt their positions in relation to the best agents, such as alpha and beta, to refine the search. This dynamic updating process is precisely defined by Eqs. (11)-(14).

$$\vec{X}(t+1) = \frac{\vec{X}_1 + \vec{X}_2 + \vec{X}_3}{3}, \quad (11)$$

$$\vec{X}_1 = \left| \vec{X}_\alpha - \vec{A}_1 \cdot \vec{D}_\alpha \right|, \quad (12)$$

$$\vec{X}_2 = \left| \vec{X}_\beta - \vec{A}_2 \cdot \vec{D}_\beta \right|, \quad (13)$$

$$\vec{X}_3 = \left| \vec{X}_\delta - \vec{A}_3 \cdot \vec{D}_\delta \right|. \quad (14)$$

In this iterative process,  $\vec{X}_\alpha$ ,  $\vec{X}_\beta$  and  $\vec{X}_\delta$  yield the three highest-ranking solutions, while Eqs. (15)-(17) are employed to compute the corresponding  $\vec{D}_\alpha$ ,  $\vec{D}_\beta$ , and  $\vec{D}_\delta$  parameters.

$$\vec{D}_\alpha = \left| \vec{C}_1 \cdot \vec{X}_\alpha - \vec{X} \right|, \quad (15)$$

$$\vec{D}_\beta = \left| \vec{C}_2 \cdot \vec{X}_\beta - \vec{X} \right|, \quad (16)$$

$$\vec{D}_\delta = \left| \vec{C}_3 \cdot \vec{X}_\delta - \vec{X} \right|. \quad (17)$$

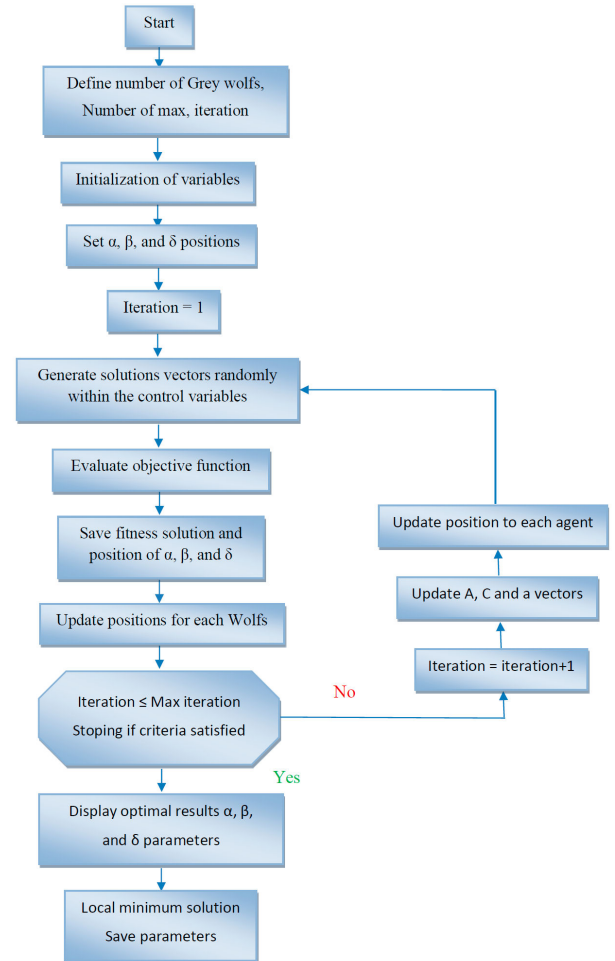


FIGURE 7. Flowchart Illustrating the Estimation of SBD Parameters Using GWO.

## Attacking prey

Gray wolves engage their prey when it ceases its movements, effectively signaling the culmination of the hunt. The mathematical model delineating this approach is encapsulated by variable  $A$ . Additionally, a decrease in  $A$  is oscillation range is implemented, as represented by equation (18). In this equation, the condition  $|A|$ , specified in condition 1, triggers the wolves' attack on their quarry.

$$A = 2 - 2 \frac{t}{\text{Max}}. \quad (18)$$

The method operates within the range of zero to the maximum number of iterations (Max), with  $t$  representing the current iteration count. Figure 7 illustrates the flowchart employed for estimating SBD parameters via the GWO algorithm [31], aligning seamlessly with the methodology detailed earlier.

## 5. Results and discussion

Table II provides an overview of the parameters utilized within the Grey Wolf Optimizer (GWO) algorithm. It specifies the lower and upper bounds for optimization concerning the parameters  $n$ ,  $R_S$ , and  $\phi_{bn}$ , setting them at [1, 10, 0.4] and [3, 100, 0.8], respectively. The dimension of this optimization problem is established as 3, signifying the total number of parameters subjected to optimization. Furthermore, the algorithm is programmed to conduct 1000 iterations employing a swarm consisting of 20 particles. To evaluate the effectiveness of the proposed GWO algorithm in determining electrical parameters, we compare the extracted parameters (specifically barrier height  $\phi_{bn}$ , series resistance  $R_S$  and ideality factor  $n$ ) of the Schottky diodes to the original values calculated using the Cheung and Cheung method,

TABLE II. GWO algorithm parameters.

Parameters	Values
Lower bound [ $n$ $R_S$ $\phi_{bn}$ ]	[1 10 0.4]
upper bound [ $n$ $R_S$ $\phi_{bn}$ ]	[3 100 0.8]
Dimension	3
Number of iterations	1000
Number of particles	20

as outlined in Table III. This comparison allows us to assess the accuracy and reliability of the GWO algorithm in identifying these electrical parameters.

Table III reveals that both methods yield ideality factors  $n$  exceeding unity. This phenomenon can be attributed to the influence of tunnel currents, encompassing thermionic field emission (TFE) and field emission (FE) mechanisms [32]. Additionally, these findings hint at the non-uniformity of the Schottky barrier height along the metal contact. This inhomogeneity likely arises from the presence of generation-recombination centers or trap centers (defect centers) at the interface of the diode structure [13, 14].

The table's electrical parameters offer valuable insights into the comparative performance of Sample A and Sample B in the domain of Schottky diodes. Particularly noteworthy is the marked improvement in Sample B's ideality factor  $n$  when contrasted with Sample A. This reduction in the ideality factor implies that Sample B exhibits a more ideal diode behavior, characterized by diminished non-idealities like tunnel currents. Consequently, Sample B may excel in facilitating the efficient transport of charge carriers across the diode junction.

Furthermore, Sample B boasts a significantly lower series resistance (RS) than Sample A, indicative of a reduced voltage drops across the diode. This diminished RS translates

TABLE III. Electrical parameters obtained from I-V curves of Au/GaN/GaAs Schottky diodes.

Parameters	Extraction method	Sample (A)	Sample (B)
$I_S$	$\text{Ln}(I/1 - \exp(-qV/kt))$	$3,51 \times 10^{-08}$	$3,42 \times 10^{-07}$
	$\text{Ln}(I/1 - \exp(-qV/kt))$	2.29	1.94
$n$	$dV/d \ln(I)$ vs. $I$	2.27	1.92
	$H(I)$ vs. $I$	-	-
	GWO	2.27	1.92
	$\text{Ln}(I/1 - \exp(-qV/kt))$	62	17
$R_S(\Omega)$	$dV/d \ln(I)$ vs. $I$	60	16.22
	$H(I)$ vs. $I$	63	16.22
	GWO	62	16.30
	$\text{Ln}(I/1 - \exp(-qV/kt))$	0.75	0.64
$\phi_{bn}(\text{eV})$	$dV/d \ln(I)$ vs. $I$	-	-
	$H(I)$ vs. $I$	0.73	0.62
	GWO	0.73	0.62
	$\text{Ln}(I/1 - \exp(-qV/kt))$	0.73	0.62

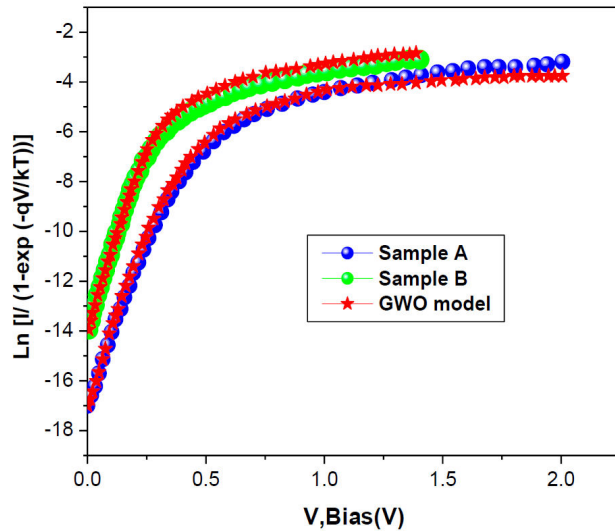


FIGURE 8. Comparison of GWO algorithm-derived I-V characteristic curves with experimental data for Schottky diodes.

into heightened overall efficiency and performance, positioning Sample B as a preferred choice for practical applications.

Moreover, the marginally lower barrier height  $\phi_{bn}$  in Sample B compared to Sample A suggests a potential enhancement in the ease of charge carrier mobility across the diode junction. These noteworthy distinctions underscore the pivotal role of material processing conditions, such as nitridation duration and GaN layer thickness, in shaping the electrical parameters of Schottky diodes. They underscore the imperative nature of optimizing these parameters to unlock the full potential of Schottky diodes for diverse electronic applications.

Notably, the parameters derived through the Grey Wolf Optimizer (GWO) method align perfectly with those obtained via the Cheung and Cheung method. This alignment attests to the GWO algorithm's exceptional ability to attain the global optimum with a remarkably high degree of accuracy, further establishing its utility in optimizing diode characteristics and performance.

Figure 8 provides a visual representation of the simulation results, comparing the evolution of experimental data  $f(V) = \text{Ln}[I/(1 - \exp(-qV)/kT)]$  with those derived

using the GWO algorithm. Clearly, the I-V characteristic curves obtained by GWO exhibit good agreement with the experimental data, further validating the accuracy and reliability of the GWO algorithm in modeling diode characteristics.

## 6. Conclusion

In this comprehensive study, we have introduced the Grey Wolf Optimization (GWO) algorithm as a powerful tool for the precise determination of the electrical parameters governing Au/GaN/GaAs Schottky diodes. The outcomes of this investigation have unveiled the remarkable efficacy of the GWO method in optimizing diode characteristics and enhancing performance.

One of the standout achievements of this research is the exceptional congruence between the parameters derived through the GWO algorithm and those obtained via the established Cheung and Cheung method. This striking alignment underscores the GWO algorithm's capacity to converge towards the global optimum with an impressive level of accuracy. Consequently, it solidifies the GWO algorithm as a robust and reliable technique for parameter estimation in Schottky diodes.

Furthermore, the presented GWO technique demonstrates notable advantages in terms of computational efficiency. Its speed and simplicity empower the utilization of the entire bias array, eliminating the need for intricate initial assumptions. Instead, it operates with a wide parameter range, offering flexibility and ease of implementation.

In conclusion, this research makes a valuable contribution to the field of diode parameter estimation by introducing the Grey Wolf Optimization (GWO) algorithm. The remarkable alignment between GWO-derived parameters and those from the Cheung and Cheung method underscores the algorithm's accuracy and reliability. Additionally, the GWO approach's computational efficiency, precision, simplicity, and adaptability position it as a promising tool for optimizing semiconductor applications. This potential opens avenues for further exploration, offering a pathway to enhance device performance and efficiency in electronic devices.

1. Bhattacharya Pallab, Semiconductor optoelectronic devices, 2nd ed. River, NJ, United States: Prentice-Hall, Inc., 1997.
2. S. M. Sze, Semiconductor Devices: Physics and Technology, vol. 2016.
3. A. Rabehi et al., Study of the characteristics current-voltage and capacitance-voltage in nitride GaAs Schottky diode, The European Physical Journal Applied Physics, vol. 72, no. 1, p. 10102, Oct. 2015, doi: 10.1051/epjap/2015150140.
4. R. C. Jaeger, Blalock N. Travis, and Blalock J. Benjamin, Microelectronic circuit design. New York: McGraw-Hill, 1997.
5. A. H. Kacha et al., Effects of the GaN layers and the annealing on the electrical properties in the Schottky diodes based on nitrated GaAs, Superlattices Microstruct, vol. 83, pp. 827-833, Jul. 2015, doi: 10.1016/j.spmi.2015.04.017.
6. G. A. Salvatore, L. Yin, and F. Dai, Biodegradable Electronics, 2023, pp. 1019-1041. doi: 10.1007/978-3-030-79827-7\_28.
7. A. Rabehi et al., Optimal Estimation of Schottky Diode Parameters Using Advanced Swarm Intelligence Algorithms, Semiconductors, vol. 54, no. 11, pp. 1398-1405, Nov. 2020, doi: 10.1134/S1063782620110214.

8. A. Rabehi et al., Optimal estimation of Schottky diode parameters using a novel optimization algorithm: Equilibrium optimizer, *Superlattices Microstruct.*, vol. 146, p. 106665, Oct. 2020, doi: 10.1016/j.spmi.2020.106665. 18
9. H. Norde, A modified forward I - V plot for Schottky diodes with high series resistance, *J Appl Phys.*, vol. 50, no. 7, pp. 5052-5053, Jul. 1979, doi: 10.1063/1.325607.
10. S. K. Cheung and N. W. Cheung, Extraction of Schottky diode parameters from forward current-voltage characteristics, *Appl Phys Lett.*, vol. 49, no. 2, pp. 85-87, Jul. 1986, doi: 10.1063/1.97359.
11. N. Karaboga, S. Kockanat, and H. Dogan, Parameter determination of the Schottky barrier diode using by artificial bee colony algorithm, in *2011 International Symposium on Innovations in Intelligent Systems and Applications, IEEE*, Jun. 2011, pp. 6-10. doi: 10.1109/INISTA.2011.5946047.
12. B. Lakehal, Z. Dibi, N. Lakhdar, A. Dendouga, and A. Benhaya, Parameter determination of Schottky -barrier diode model using genetic algorithm, in *2011 International Conference on Communications, Computing and Control Applications (CCCA), IEEE*, Mar. 2011, pp. 1-4. doi: 10.1109/CCCA.2011.6031466.
13. K. Ishaque, Z. Salam, H. Taheri, and A. Shamsudin, A critical evaluation of EA computational methods for Photovoltaic cell parameter extraction based on two diode model, *Solar Energy*, vol. 85, no. 9, pp. 1768-1779, Sep. 2011, doi: 10.1016/j.solener.2011.04.015.
14. O. Ya. Olikh, Review and test of methods for determination of the Schottky diode parameters, *J Appl Phys.*, vol. 118, no. 2, Jul. 2015, doi: 10.1063/1.4926420.
15. S. Mirjalili, S. M. Mirjalili, and A. Lewis, Grey Wolf Optimizer, *Advances in Engineering Software*, vol. 69, pp. 46-61, Mar. 2014, doi: 10.1016/j.advengsoft.2013.12.007.
16. A. Abushawish and A. Jarndal, Hybrid particle swarm optimization < scp > - < /scp > grey wolf optimization based < scp > small-signal < scp > modeling applied to < scp > GaN < /scp > devices, *International Journal of RF and Microwave Computer-Aided Engineering*, vol. 32, no. 5, May 2022, doi: 10.1002/mmce.23081.
17. H. Bencherif, L. Dehimi, F. Pezzimenti, and F. G. Della Corte, Improving the efficiency of a-Si:H/c-Si thin heterojunction solar cells by using both antireflection coating engineering and diffraction grating, *Optik (Stuttg)*, vol. 182, pp. 682-693, Apr. 2019, doi: 10.1016/j.ijleo.2019.01.032.
18. H. Dogan, Parameter Estimation of Al/p-Si Schottky Barrier Diode Using Different Meta-Heuristic Optimization Techniques, *Symmetry (Basel)*, vol. 14, no. 11, p. 2389, Nov. 2022, doi: 10.3390/sym14112389.
19. L. Bideux, G. Monier, V. Matolin, C. Robert-Goumet, and B. Gruzza, XPS study of the formation of ultrathin GaN film on GaAs(100), *Appl Surf Sci.*, vol. 254, no. 13, pp. 4150-4153, Apr. 2008, doi: 10.1016/j.apsusc.2007.12.058.
20. G. Monier et al., Passivation of GaAs(001) surface by the growth of high quality c-GaN ultra-thin film using low power glow discharge nitrogen plasma source, *Surf Sci.*, vol. 606, no. 13-14, pp. 1093-1099, Jul. 2012, doi: 10.1016/j.susc.2012.03.006. 19
21. C. A. Hernández-Gutiérrez et al., Characterization of n-GaN / p-GaAs NP heterojunctions, *Superlattices Microstruct.*, vol. 136, p. 106298, Dec. 2019, doi: 10.1016/j.spmi.2019.106298.
22. S. Suandon, S. Sanorpim, K. Yoodee, and K. Onabe, Effect of growth temperature on polytype transition of GaN from zincblende to wurtzite, *Thin Solid Films.*, vol. 515, no. 10, pp. 4393-4396, Mar. 2007, doi: 10.1016/j.tsf.2006.07.109.
23. A. Rabehi et al., Current-Voltage, Capacitance-Voltage-Temperature, and DLTS Studies of Ni—6H-SiC Schottky Diode, *Semiconductors*, vol. 55, no. 4, pp. 446-454, Apr. 2021, doi: 10.1134/S1063782621040138.
24. H. Helal et al., A new model of thermionic emission mechanism for non-ideal Schottky contacts and a method of extracting electrical parameters, *The European Physical Journal Plus*, vol. 135, no. 11, p. 895, Nov. 2020, doi: 10.1140/epjp/s13360-020-00916-5.
25. Rabehi Abdelaziz et al., Modeling the Abnormal Behavior of the 6H-SiC Schottky Diode Using Lambert W Function, *JOURNAL OF NANO- AND ELECTRONIC PHYSICS*, vol. 14, no. 6, pp. 6032-6036, 2022.
26. H. Helal et al., A study of current-voltage and capacitance-voltage characteristics of Au/n-GaAs and Au/GaN/n-GaAs Schottky diodes in wide temperature range, *International Journal of Numerical Modelling: Electronic Networks, Devices and Fields*, vol. 33, no. 4, Jul. 2020, doi: 10.1002/jnm.2714.
27. J. H. Werner, Schottky barrier and pn-junction I/V plots ? Small signal evaluation, *Applied Physics A Solids and Surfaces*, vol. 47, no. 3, pp. 291-300, Nov. 1988, doi: 10.1007/BF00615935.
28. K. Wang and M. Ye, PARAMETER ESTIMATION OF SCHOTTKY-BARRIER DIODE MODEL BY PARTICLE SWARM OPTIMIZATION, *International Journal of Modern Physics C*, vol. 20, no. 05, pp. 687-699, May 2009, doi: 10.1142/S0129183109013911.
29. K. Wang and M. Ye, Parameter determination of Schottky-barrier diode model using differential evolution, *Solid State Electron.*, vol. 53, no. 2, pp. 234-240, Feb. 2009, doi: 10.1016/j.sse.2008.11.010.
30. M. Pradhan, P. K. Roy, and T. Pal, Grey wolf optimization applied to economic load dispatch problems, *International Journal of Electrical Power & Energy Systems*, vol. 83, pp. 325-334, Dec. 2016, doi: 10.1016/j.ijepes.2016.04.034.
31. H. Doğan, Parameter Estimation of Al/p-Si Schottky Barrier Diode Using Different Meta-Heuristic Optimization Techniques, *Symmetry (Basel)*, vol. 14, no. 11, p. 2389, Nov. 2022, doi: 10.3390/sym14112389.
32. E. Özavcı, S. Demirezen, U. Aydemir, and S. Altındal, A detailed study on current-voltage characteristics of Au/n-GaAs in wide temperature range, *Sens Actuators A Phys.*, vol. 194, pp. 259-268, May 2013, doi: 10.1016/j.sna.2013.02.018.